ISSN 1392–1207. MECHANIKA. 2016 Volume 22(1): 59–64

Experimental investigation and numerical simulation of the friction stir spot welding process

S. Kilikevičius*, R. Česnavičius, P. Krasauskas***, R. Dundulis****, J. Jaloveckas*******
**Kaunas University of Technology, Studentų 56, 51424 Kaunas, Lithuania, E-mail: sigitas.kilikevičius@ktu.lt*
***Kaunas University of Technology, Studentų 56, 51424 Kaunas, Lithuania, E-mail: ramunas.cesnavicius@ktu.lt*
****Kaunas University of Technology, Studentų 56, 51424 Kaunas, Lithuania, E-mail: povilas.krasauskas@ktu.lt*
*****Kaunas University of Technology, Studentų 56, 51424 Kaunas, Lithuania, E-mail: romualdas.dundulis@ktu.lt*
******Kaunas University of Technology, Studentų 56, 51424 Kaunas, Lithuania, E-mail: julius.jaloveckas@stud.ktu.lt*

crossref http://dx.doi.org/10.5755/j01.mech.22.1.6029

1. Introduction

Friction stir spot welding (FSSW) is a metal joining technique used to replace conventional joining processes such as riveting, resistance spot welding and fastening. Thin-walled steel plates structures usually are joined using electric resistance spot welding, but this type of welding is ineffective and complicated for the light-weighted alloys due to the lower electrical properties of the alloys and more expensive compared to the steel welding [1, 2].

A friction stir spot weld is formed by plunging rotating tool into two plates, stirring for a short period of time and then retracting it back. Due to the frictional heat generated between the tool and the plates, the stirred materials are softened, which allows them to be intermixed by the tool, in this way a partial metallurgical bond is created. The strength of the joint depends mainly on the geometry of the tool and the conditions of welding process [1, 3].

The papers [3, 4] present experimental investigations on the influence of the tool geometry on stir spot weld hook formation and static strength of FSSW joints, still, there are not a lot of studies dealing with the influence of the tool rotation speed, tool plunge rate and dwell time on the FSSW process.

The numerical simulation of the FSSW process is a complicated task conditioned by a lot of conventionalities and uncertainties as well as highly dependent on various factors such as material properties, welding process conditions, geometrical parameters of the tool, etc. During FSSW, high strain and strain rate takes place resulting in a complicated problem involving non-linear material behaviour, excessive mesh distortion and the need for high computational resources; therefore, a numerical simulation of friction drilling for each new material is complicated and specific.

Awang et al. [5] presented a simulation of FSSW using the finite element method (FEM). Adaptive meshing and advection schemes, which makes it possible to maintain mesh quality under large deformations, was used to simulate the material flow and temperature distribution. Temperature distribution in the workpiece using the adaptive meshing scheme and the Johnson-Cook material law was analysed by Sathiya et al. [6]. The effect of tool geometry on the plastic flow and material mixing during FSSW was investigated using the particle method approach by Hirasawa et al. [7]. However, these papers did not investigate the welding force which occurs during FSSW.

The welding force, the temperature distribution in the welding region and the mechanical properties of the joints were investigated using experimental and FEM techniques by D'Urso [8, 9]. However, a 2D approach used for the simulation of a 3D problem was used in the FEM model. The welding force and the temperature distribution during the plunge stage of FSSW were investigated by Mandal et al. [10] conducting an experiment and a FEM simulation. However, only the plunge stage was analysed using just one plate as a workpiece.

Another approach for FSSW simulation is the computational fluid dynamics method [11, 12]. However, it is difficult to estimate metal properties of the plastic deformation behaviour applying fluid models for FSSW.

The aims of this paper is to carry out FSSW experiments using aluminium alloy 5754 in order to analyse the welding force under different welding regimes, conduct a FEM simulation of the process and compare the results.

3. Experimental setup

The FSSW experiment was carried out using aluminium alloy 5754 plates with 1.0 mm in thickness.

a

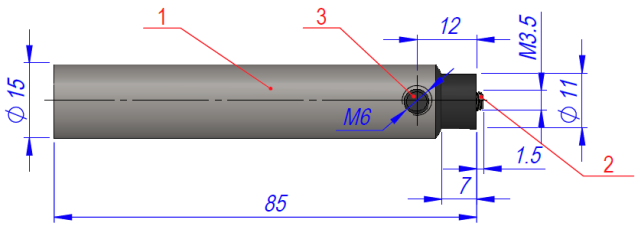

b

Fig. 1 Three-dimension view of the FSSW tool (a) and its dimensions (b): *1* - shoulder; *2* - pin; *3* - screw for fixing pin in the shoulder

The experiment was carried out on a CNC milling

machine “DMU-35M” with a “Sinumerik 810D/840D” controller and “ShopMill” software using a high speed steel tool with special thread of M3.5. The tool consists of three parts: a 2 mm length left hand M3.5 thread pin *1* which is made of tool steel X37CrMoV5-1 EN ISO 4957: 2002 and hardened to 50 HRC, a shoulder *2* with a body diameter of 11 mm and a concavity of 5° and a fixing screw *3*. The dimensions of the FSSW tool shape and the 3D model are shown in Fig. 1.

The axial force was measured using a universal laboratory charge amplifier Kistler type 5018A and a press force sensor Kistler type 9345B mounted on the CNC table. Measuring ranges of the sensor for force: -10…10 kN; sensitivity: ≈-3.7 pC/N. The amplifier converts the charge signal from the piezoelectric pressure sensor into a proportional output voltage.

The variation of the axial force was recorded to a computer using a “PicoScope 4424” oscilloscope and “PicoScope 6” software. The experimental setup is shown in Fig. 2.

a b

Fig. 2 Setup of FSSW experiment: a - overall view of the test-bench; b - clamping – measuring device

3. Experimental investigation

The friction stir spot welding experiments were carried out welding two identical plates of the same material (aluminium alloy 5754 was used for the experiments).

The chemical composition of aluminium alloy 5754 is: Si 0-0.4%, Fe 0-0.4%, Mn 0-0.5%, Mg 2.6-3.6%, Zn 0-0.2, Cu 0-0.1%, Ti 0-0.15%, Cr 0-0.3%; Al (Balance).

Plates with dimensions 150x60x1 mm were fixed on a press force device using clamping jaws. The examples of friction stir spot welds are shown in Fig. 3.

Fig. 3 Examples of stir spot welds

In order to investigate the influence of the tool rotation speed on the welding force, two were welded under spindle speed *S* values of 2000, 2500 and 3000 rpm and tool feed rate *F* values of 60, 100 and 140 mm/min. The results showed that an increase in the feed rate results in an increase in the welding axial force (Fig. 4).

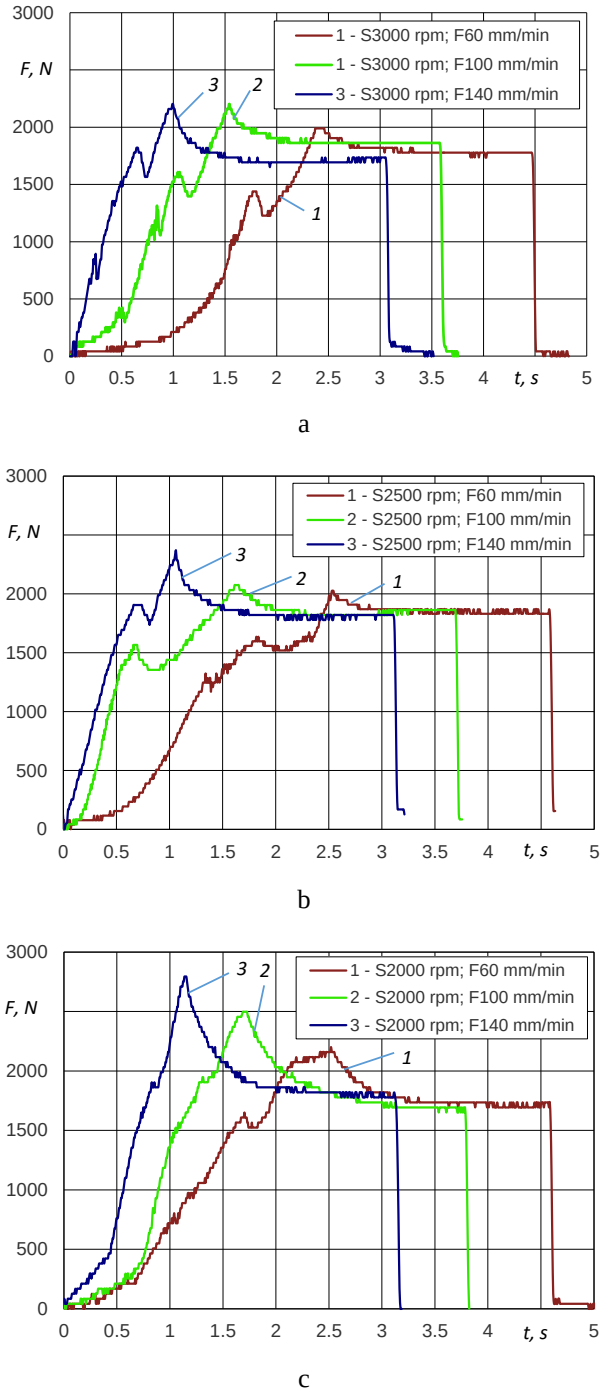

Fig. 4 Influence of friction stir spot welding tool feed rate on the axial force, under different spindle speed: a - 3000 rpm; b - 2500 rpm; c - 2000 rpm

Fig. 4 shows that the welding process could be divided into three phases: the first – tool pin penetration and plunging into the sheet with a predicted spot depth; the second – dwell (stirring) and the third – rapid tool retraction. As it is seen from the graph, the welding force reaches its peak value when the shoulder face touches the upper plate surface and then, during the dwell time, slightly decreases and after that, the axial welding force remains quite stable till the tool retraction.

4. Theoretical background of FSSW simulation

In case of FSSW, heat is generated from two sources: plastic energy dissipation due to the shear deformation and heating due to the friction in the tool and workpiece contact zone.

The governing equation describing the heat transfer during FSSW can be expressed as follows [13]:

$$\rho c \frac{\partial T}{\partial t} = \left[k_x \frac{\partial^2 T}{\partial x^2} + k_y \frac{\partial^2 T}{\partial y^2} + k_z \frac{\partial^2 T}{\partial z^2} \right] + \dot{q}_f , \quad (1)$$

where ρ is the material density; c is the specific heat, T is the temperature, t is the time, k is the heat conductivity in x, y, and z coordinates; $\dot{q}_f$ is the heat generated by the friction between the tool and the workpiece, it is expressed:

$$\dot{q}_f = \int_0^{T_f} \omega \, dT_f , \quad (2)$$

where ω is the angular velocity of the tool and T_f is the friction moment in the contact zone.

For the finite element method simulation the temperature and strain rate dependent Johnson-Cook model was used [14]. In this case, the flow stress is expressed:

$$\bar{\sigma} = \left(A + B \left(\bar{\varepsilon}_{pl} \right)^n \right) \left[1 + C \ln \frac{\dot{\bar{\varepsilon}}_{pl}}{\dot{\varepsilon}_0} \right] \left(1 - \left(\frac{T - T_{room}}{T_{melt} - T_{room}} \right)^m \right) , \quad (3)$$

where parameter A is the initial yield strength of the material at room temperature, B is the hardening modulus; C is the parameter representing strain rate sensitivity; $\bar{\varepsilon}_{pl}$ is the effective plastic strain; $\dot{\bar{\varepsilon}}_{pl}$ is the effective plastic strain rate $\dot{\varepsilon}_0$ is the reference strain rate; n is the strain hardening exponent; m is the parameter which evaluates thermal softening effect, T_{melt} and T_{room} are the material melting and room temperatures.

5. Computational model for FSSW

A three-dimensional geometry model of the tool and the workpieces was created in SolidWorks software and imported in ABAQUS/EXPLICIT software. The workpieces were created as 15x15x1 mm plates. Only these elements of the tool were modelled which can be in contact with the workpieces (Fig. 5).

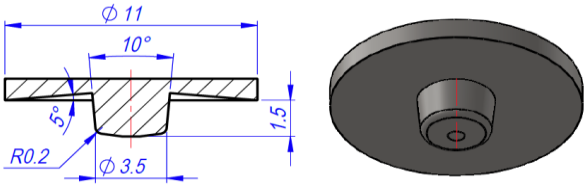

Fig. 5 Dimensions and 3D model of the tool

The adaptive meshing technique was used in this study, carrying it out for every ten increments and performing five mesh sweeps per adaptive mesh increment. The tool was meshed using element type C3D10MT due to its complex shape and the plates were meshed using element type C3D8RT. An element size of 0.3 mm was used for the tool and an element size of 0.15 mm was used for the plates. 8 layers of elements through the thickness were generated in each of the plates. The mesh of each plate contained 63368 elements and the mesh of the tool contained 32417 elements. The mesh is shown in Fig. 6.

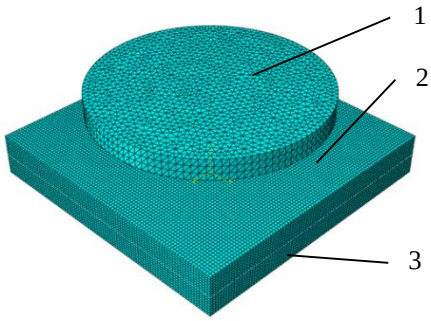

Fig. 6 Finite element mesh: *1* - tool; *2* - upper plate; *3* - lower plate

In order to save computational time, the mass scaling technique was used that modifies the densities of the materials in the model and improves the computational efficiency [15], obtaining a stable time increment of at least 0.0001 s step time.

In the normal direction, the contacting surfaces of the components were assumed to be hard in which pressure-overclosure relationships were used to avoid the penetration of slave nodes into the master surface.

It was assumed that 100% of dissipated energy caused by friction between the parts was converted to heat. The temperature dependent friction coefficient μ of aluminium and steel used in this study is presented in Table 1 [5]. The friction coefficient was set to 0 at the melting temperature of aluminium alloy 5754.

Table 1

Temperature dependent friction coefficient of aluminium and steel

Temperature (K)	Friction coefficient
273	0.61
307.7	0.545
366.3	0.359
420.5	0.255
483.6	0.244
533	0.147
588.6	0.135
644.1	0.02
699.7	0.007

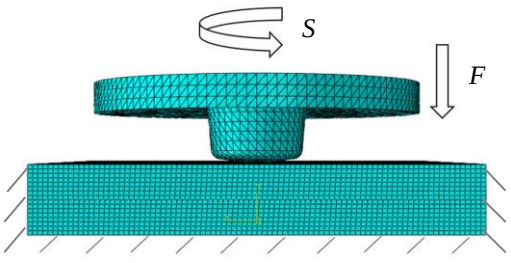

Fig. 7 Boundary conditions

The boundary conditions (Fig. 7) were set as follow: the bottom surface and all four sides of the lower plate as well as all the sides of the upper plate were restrained in all degree of freedom; the top surface of the upper plate was under free convection with the convection coefficient of 30 W/m^{2}K; the ambient air temperature and the initial temperature of the workpiece were set to 295 K (22ºC).

Table 2

Mechanical properties and the Johnson-Cook parameters for aluminium alloy 5754

Parameter	Units	Value
Young modulus, E	GPa	70.5
Poisson's ratio, v	-	0.33
Density, ρ	Kg/m^3	2680
Melting temperature, θ_{melt}	K	873
Specific heat capacity	J/(kgK)	897
Thermal conductivity	W/(mK)	132
Initial yield strength A	MPa	67.456
Hardening modulus B	MPa	471.242
Strain hardening exponent n	-	0.424
Thermal softening exponent m	-	2.519
Strain rate constant C	-	0.003

Material properties and the Johnson-Cook parameters used for the FSSW simulation are presented in Table 2 [16].

Element deletion is essential for material separation in FSSW, it allows elements to separate and the tool to penetrate the workpieces [17]. In this study, the criterion to delete an element is based on the value of the equivalent plastic strain, which was suitable for the high strain-rate deformation in FSSW [15]. The equivalent plastic strain threshold was set to the maximum value possible while maintaining convergence in the FSSW simulation.

6. Numerical simulation and comparison to the experimental results

The simulation of the FSSW process was carried out and results were obtained.

Fig. 8 shows how the equivalent plastic strain changes during the FSSW process under spindle speed S = 3000 rpm and feed rate F = 140 mm/min. Throughout the whole process, the maximum value of equivalent plastic strain was 2.34.

Fig. 9 shows how the temperature changes during the FSSW process. The simulation showed that the temperature has a tendency to increase during the dwell time. The maximum value was 746 K (473°C) after approximately 2 seconds of dwell time.

Fig. 8 and Fig 9 show that the shape of the spot weld is close to the actual shape obtained by the experiments (Fig. 3).

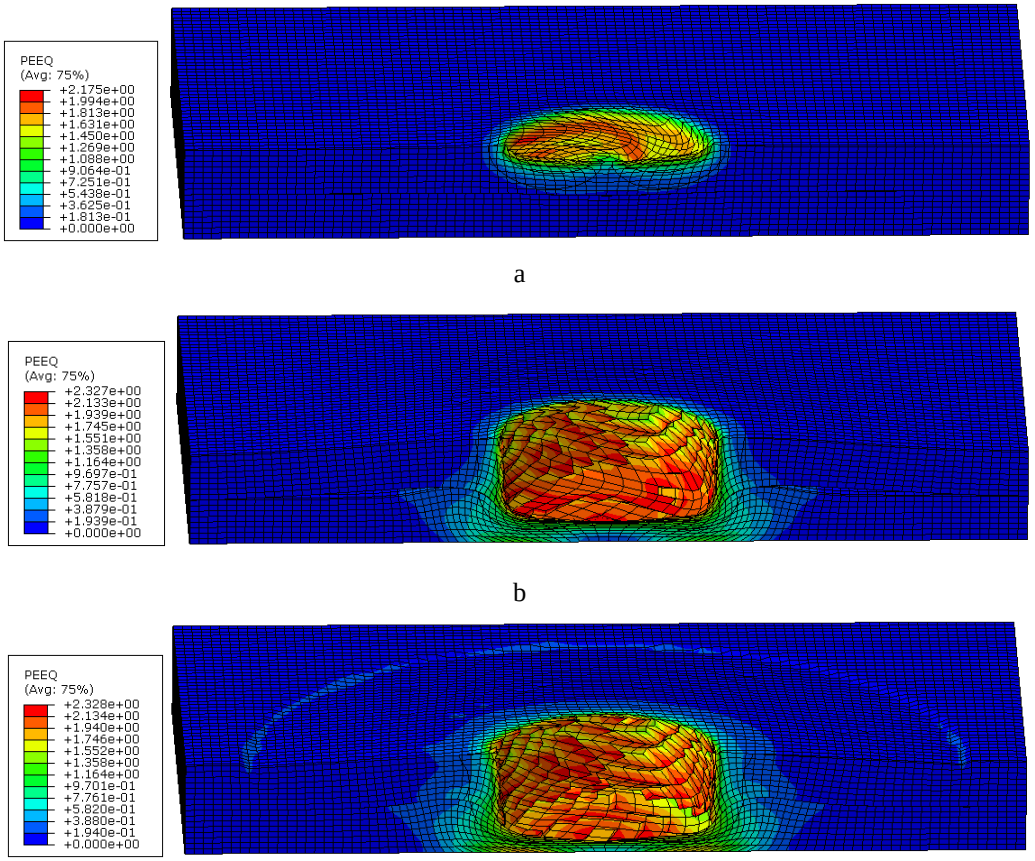

Fig. 8 Equivalent plastic strain at various distances of tool travel: a - 0.29 mm; b - 1.53 mm; c - 1.71 mm, when S = 3000 rpm and F = 140 mm/min

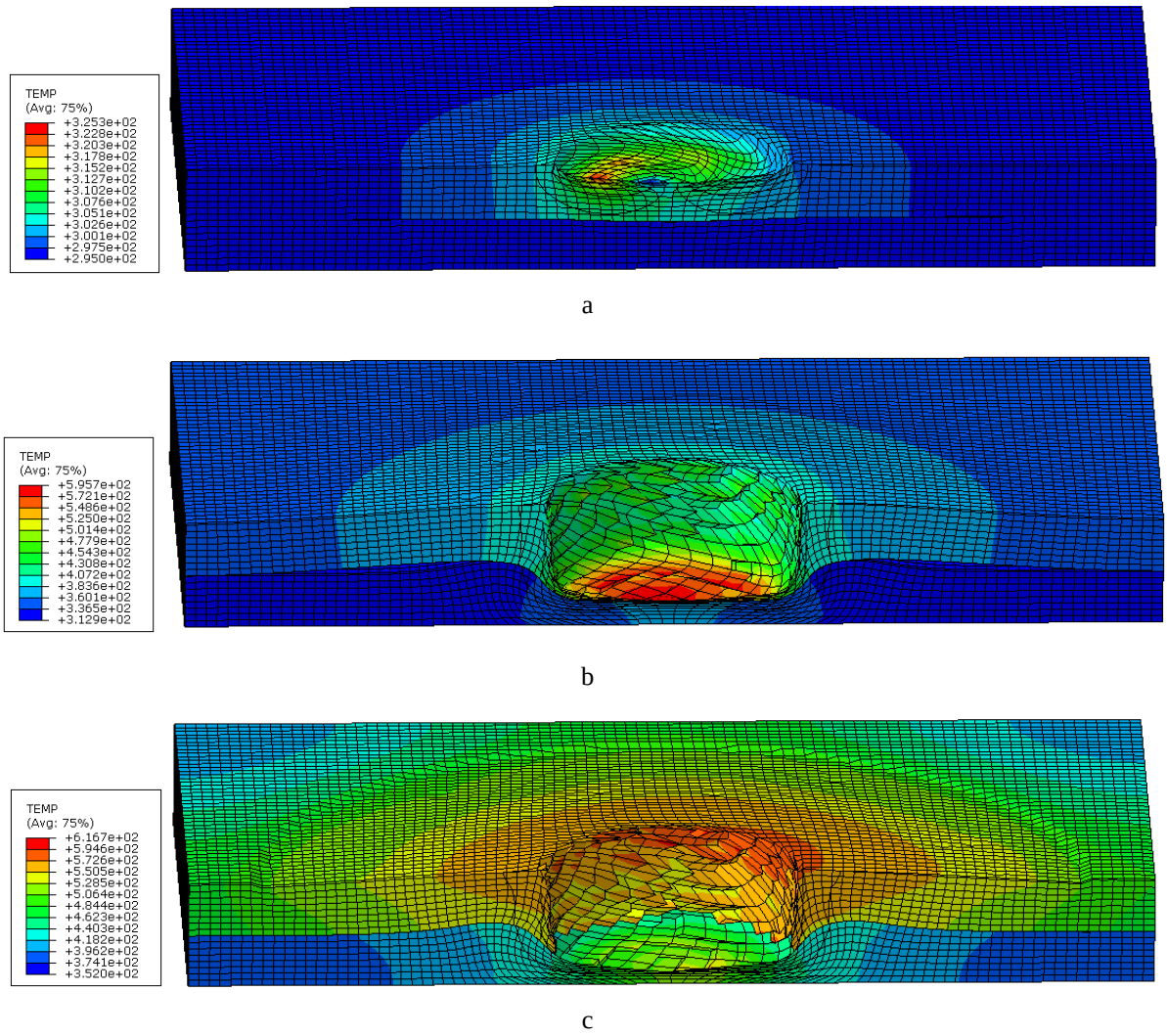

Fig. 9 Temperature (units are in K) at various distances of tool travel: a - 0.29 mm; b - 1.53 mm; c - 1.71 mm, when S = 3000 rpm and F = 140 mm/min

The variation of the experimental and the simulated welding force over time is presented in Fig.10. Compared to the experiments, the FEM simulation showed a more distinct increase of the welding force at that instant of time when the shoulder face touches the upper plate surface. However, the trends of the experimental and the simulated welding force variation over time are quite similar and this shows that the presumptions taken in the simulation are reasonable and the FEM model quite realistically defines the FSSW process.

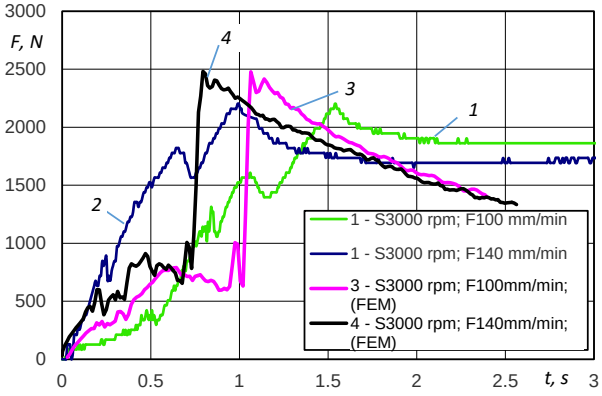

Fig. 10 Variation of the experimental and the simulated welding force

7. Conclusions

An experimental analysis and a numerical simulation of the friction stir spot welding process on aluminium alloy 5754 plates were carried out.

The experiments showed that an increase in the feed rate results in an increase in the welding axial force. It was observed that the welding force reaches its peak value when the shoulder face touches the upper plate surface and then, during the dwell time, slightly decreases and after that, the axial welding force remains quite stable till the tool retraction.

The simulation showed that the maximum value of equivalent plastic strain reached 2.34 under spindle speed S = 3000 rpm and feed rate F = 140 mm/min. The temperature has a tendency to increase during the dwell time. The maximum value was 746 K (473°C) after approximately 2 seconds of dwell time. The shape of the spot weld in the simulation is close to the actual shape obtained by the experiments. Compared to the experiments, the FEM simulation showed a more distinct increase of the welding force at that instant of time when the shoulder face touches the upper plate surface. However, the trends of the experimental and the simulated welding force variation over time are quite similar.

The results of the study show that the presumptions taken in the simulation are reasonable and the model quite realistically defines the FSSW process. The FEM model could be useful for prediction of rational FSSW regimes in order to lower welding forces and, as a consequence, to decrease tool wear.

References

1. **Barlas, Z.** 2015. Effect of friction stir spot weld parameters on Cu/CuZn30 bimetal joints, Springer. The International Journal of Advanced Manufacturing Technology 80: 161-170. http://dx.doi.org/10.1007/s00170-015-6998-1.
2. **Klobčar, D.; Tušek, J.; Skumavc, A.; Smolej, A.** 2014. Parametric study of friction stir spot welding of aluminum alloy 5754, Metalurgija 53(1): 21-24.
3. **Badarinaryan, H.; Shi, Y.; Li, X.; Okamoto, K.** 2009. Effect of tool geometry on hook formation and static strength of friction stir spot welded aluminum 5754-O sheets, International Journal of Machine Tools & Manufacture 49 814-823. http://dx.doi.org/10.1016/j.ijmachtools.2009.06.001.
4. **Cox, C.D.; Gibson, B.T.; Straus, A.M.; Cook, G.E.** 2012. Effect of pin length and rotation rate on the tensile strength of a friction stir spot-welded Al alloy: A contribution to automated production 27(4): 472-478. http://dx.doi.org/10.1080/10426914.2011.585503.
5. **Awang, M., et al.** 2005. Thermo-mechanical modeling of friction stir spot welding (FSSW) process: use of an explicit adaptive meshing scheme, SAE 2005 World Congress, Apr., vol. 13. http://dx.doi.org/10.4271/2005-01-1251.
6. **Sathiya, P., et al.** 2008 Temperature distribution modeling of friction stir spot welding of AA 6061-T6 using finite element technique, Multidiscipline Modeling in Materials and Structures 4.1: 1-14. http://dx.doi.org/10.1163/157361108783470397.
7. **Hirasawa, S., et al.** 2010. Analysis of effect of tool geometry on plastic flow during friction stir spot welding using particle method, Journal of Materials Processing Technology 210.11: 1455-1463. http://dx.doi.org/10.1016/j.jmatprotec.2010.04.003.
8. **D'Urso, G.** 2015. Thermo-mechanical characterization of friction stir spot welded AA6060 sheets, Experimental and FEM analysis Journal of Manufacturing Processes 09/2014; 17: 108-119. http://dx.doi.org/10.4028/www.scientific.net/KEM.651-653.147210.1016/j.jmapro.2014.08.004.
9. **D'Urso, G., and Giardini C.** 2015. Thermo-mechanical characterization of Friction Stir Spot Welded sheets: experimental and FEM comparison between AA6060 and AA7050 alloys. Key Engineering Materials., vols. 651-653: 1472-1479, http://dx.doi.org/10.4028/www.scientific.net/KEM.651-653.1472.
10. **Mandal, S., Rice, J., and Elmustafa, A.A.** 2008. Experimental and numerical investigation of the plunge stage in friction stir welding, Journal of materials processing technology 07/2008; 203.1: 411-419. http://dx.doi.org/10.1016/j.jmatprotec.2007.10.067.
11. **Gerlich, A., et al.** 2005. Numerical modeling of FSW spot welding: preliminary results, Friction Stir Welding and Processing III as held at the 2005 TMS Annual Meeting.
12. **Dickerson, T., Shi, Q., and Shercli, H.R.** 2004. Modelling the Friction Stir Welding of aerospace alloys, 5th International Symposium on Friction Stir Welding, Metz, France.
13. **Miller, S.F. Shih, A.J.** 2007. Thermo-mechanical Finite Element Modelling of the Friction Drilling Process, Journal of Manufacturing Science and Engineering 129: 531-538. http://dx.doi.org/10.1115/1.2716719.
14. **Johnson, G.; Cook, W.** 1983. A Constitutive Model and Data for Metals Subjected to Large Strains, High Strain Rates and High Temperatures, Proceeding of the 7th Int. Symp. On Ballistics, The Hague, the Netherlands: 1-7.
15. Abaqus Theory Manual, version 6.2, Hibbit, Karlsson & Sorensen, Inc., 2001.
16. **Smerd, R., et al.** 2005. High strain rate tensile testing of automotive aluminum alloy sheet, International Journal of Impact Engineering 12/2005; 32.1: 541-560. http://dx.doi.org/10.1016/j.ijimpeng.2005.04.013.
17. **Servis, D., and Manolis S.** 2006. Implementation of the T-failure criterion in finite element methodologies. Computers & structures 84.3: 196-214. http://dx.doi.org/10.1016/j.compstruc.2005.09.011.

S. Kilikevičius, R. Česnavičius, P. Krasauskas,
R. Dundulis, J. Jaloveckas

EXPERIMENTAL INVESTIGATION AND NUMERICAL SIMULATION OF THE FRICTION STIR SPOT WELDING PROCESS

S u m m a r y

This paper presents an experimental analysis and a numerical simulation of the friction stir spot welding (FSSW) process on aluminium alloy 5754 plates. The experiments were done in order to analyse the influence of different welding regimes on the welding force. The simulation of the FSSW process was carried out and the equivalent plastic strain, temperature and welding force were obtained. The shape of the spot weld in the simulation is close to the actual shape obtained by the experiments. The trends of the experimental and the simulated welding force variation over time are quite similar The obtained results of the presented study lead to a conclusion that the presumptions taken in the simulation are reasonable and the model quite realistically defines the FSSW process. The FEM model could be useful for prediction of rational FSSW regimes in order to lower welding forces and, as a consequence, to decrease tool wear.

Keywords: friction stir spot welding, welding force, simulation.

Received November 26, 2015
Accepted January 19, 2016